Understanding CO_2 Plume Dynamics and Trapping Mechanisms Under Relative Permeability Uncertainty in Geological Carbon Storage

Introduction

The performance and security of CO_2 storage projects depend fundamentally on accurate predictions of multiphase flow behavior in the subsurface. Among the key parameters governing these processes, relative permeability plays a central role because it controls CO_2 injectivity, plume migration, residual trapping, solubility trapping, and long-term containment. However, laboratory special core analysis (SCAL) data for supercritical CO_2–brine systems remain limited and often exhibit significant variability. As a result, uncertainty in relative permeability functions directly translates into uncertainty in storage capacity estimates, plume geometry predictions, and long-term risk assessments.

This study investigates how uncertainty in CO_2–brine relative permeability influences CO_2 plume evolution and trapping mechanisms in geological CO_2 storage. A comprehensive SCAL-based modeling workflow was developed to generate uncertainty-bounded primary drainage and imbibition relative permeability curves. These curves were implemented in a compositional reservoir simulation model to evaluate the propagation of relative permeability uncertainty into plume development, injectivity, and long-term trapping performance over injection and post-injection periods.

Methods

Three relative permeability curves for both primary drainage and imbibition with uncertainty range of optimistic, pessimistic, and base case are adopted from recent study by Akbar et al. (2026) as exhibited in Figure 1. These curves are implemented to in a 3D compositional reservoir simulation framework. The static and dynamic reservoir models were developed using the integrated reservoir simulation platform tNavigator. The simulations were conducted on a synthetic saline aquifer model adapted from Jenei et al. (2025), with a lateral grid spacing of 25 × 25 m and a vertical resolution of 4 m. Reservoir conditions were maintained at 200 bar and 100 °C to ensure supercritical CO_2 behavior throughout the simulation. The formation was assumed to be initially fully saturated with brine at a salinity of 10,000 ppm.

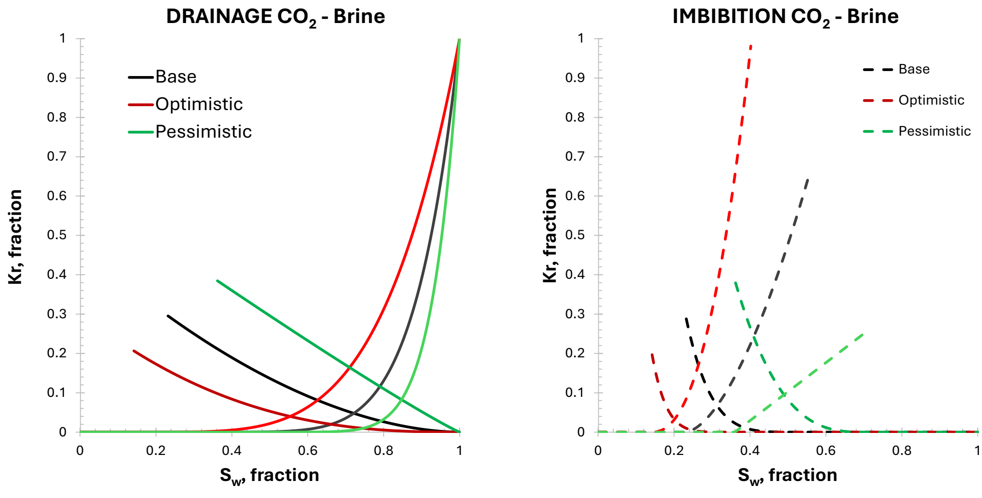

***Figure 1** Relative Permeability Uncertainty for both Primary Drainage (left) and imbibition (right).*

Pure CO_2 was injected through a single vertical well at a constant rate of 100,000 m^3/day over a two-year injection period. This was followed by a 1,000-year post-injection simulation to evaluate long-term plume behavior and trapping processes. Three relative permeability scenarios—base case, optimistic, and pessimistic—derived from the SCAL-based uncertainty modeling were implemented in the simulations. The modeling framework enabled assessment of CO_2 plume evolution, injectivity, and the relative contributions of mobile, residually trapped, and dissolved CO_2 under varying relative permeability assumptions.

Results

Simulation results demonstrate that relative permeability uncertainty exerts a first-order control on CO_2 plume geometry, migration dynamics, and long-term trapping efficiency. The spatial evolution of the plume is illustrated in Figures 2 and 3, which present cross-sectional views of CO_2 plume evolution with brine mass density distribution and free-phase CO_2 saturation distribution at the end of injection (2 years) and during the post-injection period (300 and 1,000 years).

At the end of the two-year injection period, clear differences in plume characteristics are already evident among the three scenarios (Figure 2 and Figure 3). The pessimistic case, characterized by higher CO_2 endpoint relative permeability, produces a broader and more vertically extended plume due to elevated gas mobility and earlier phase connectivity. In contrast, the optimistic case exhibits a more compact and vertically confined plume, reflecting reduced CO_2 mobility and delayed gas-phase connectivity. The base case displays intermediate behavior.

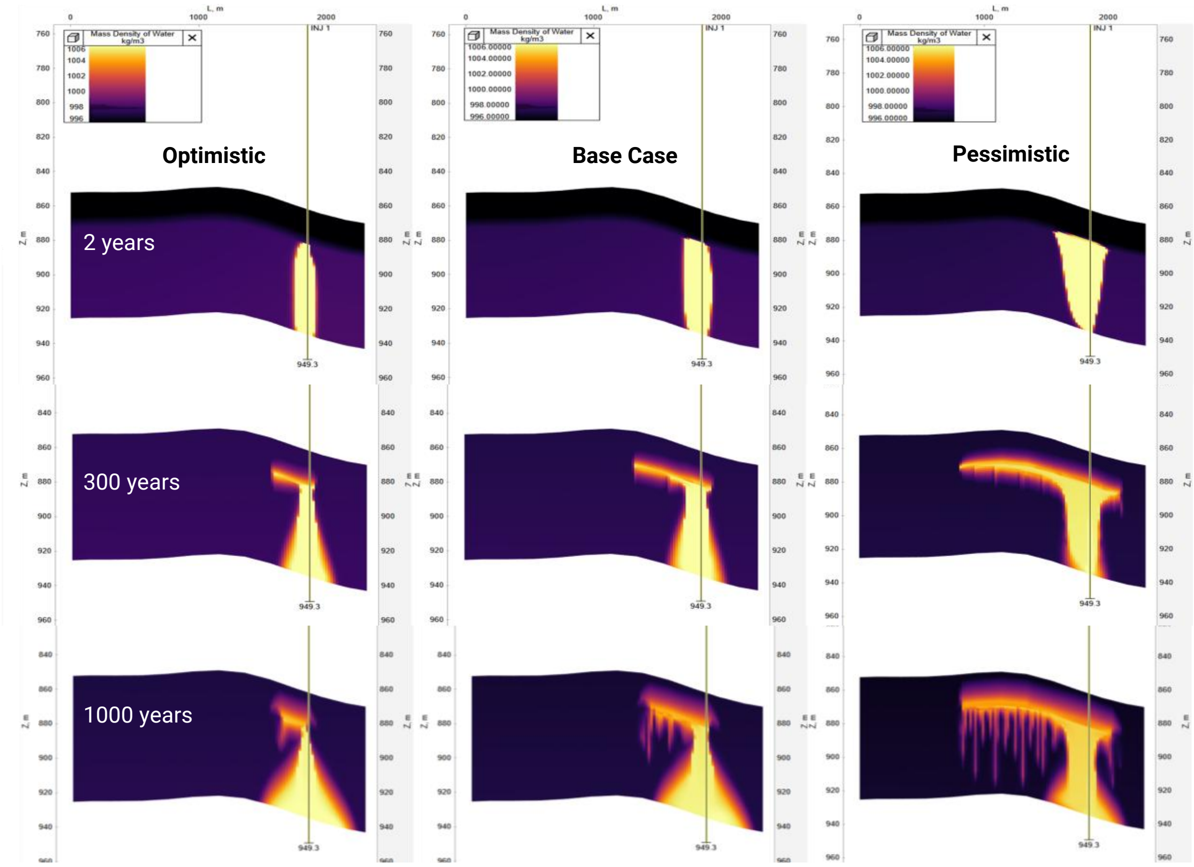

Figure 2 *Simulated CO_2 plume evolution and brine mass density distribution for optimistic, base-case, and pessimistic relative permeability scenarios at the end of 2 years of injection and after 300 and 1,000 years of post-injection migration.*

During the post-injection period, buoyancy-driven redistribution amplifies these differences. After 300 years, the pessimistic scenario develops a laterally extensive gravity tongue beneath the caprock, indicating sustained CO_2 mobility and weaker capillary immobilization. The optimistic scenario, however, retains a thicker and more localized plume, suggesting stronger residual trapping and reduced lateral migration. Enhanced CO_2–brine contact in this case also promotes greater dissolution into the aqueous phase.

After 1,000 years, the divergence between scenarios becomes more pronounced. The pessimistic model maintains the largest plume footprint and the highest fraction of mobile CO_2, indicating reduced long-term containment security. Conversely, the optimistic scenario exhibits a compact plume core with a greater proportion of residually trapped and dissolved CO_2, reflecting improved capillary and solubility trapping efficiency. The base case remains intermediate in both spatial extent and trapping partitioning.

Overall, the results highlight that variations in relative permeability parameters alone can generate substantial differences in plume evolution and storage performance over millennial timescales, underscoring their critical importance in CCS uncertainty assessment and risk-informed reservoir modeling.

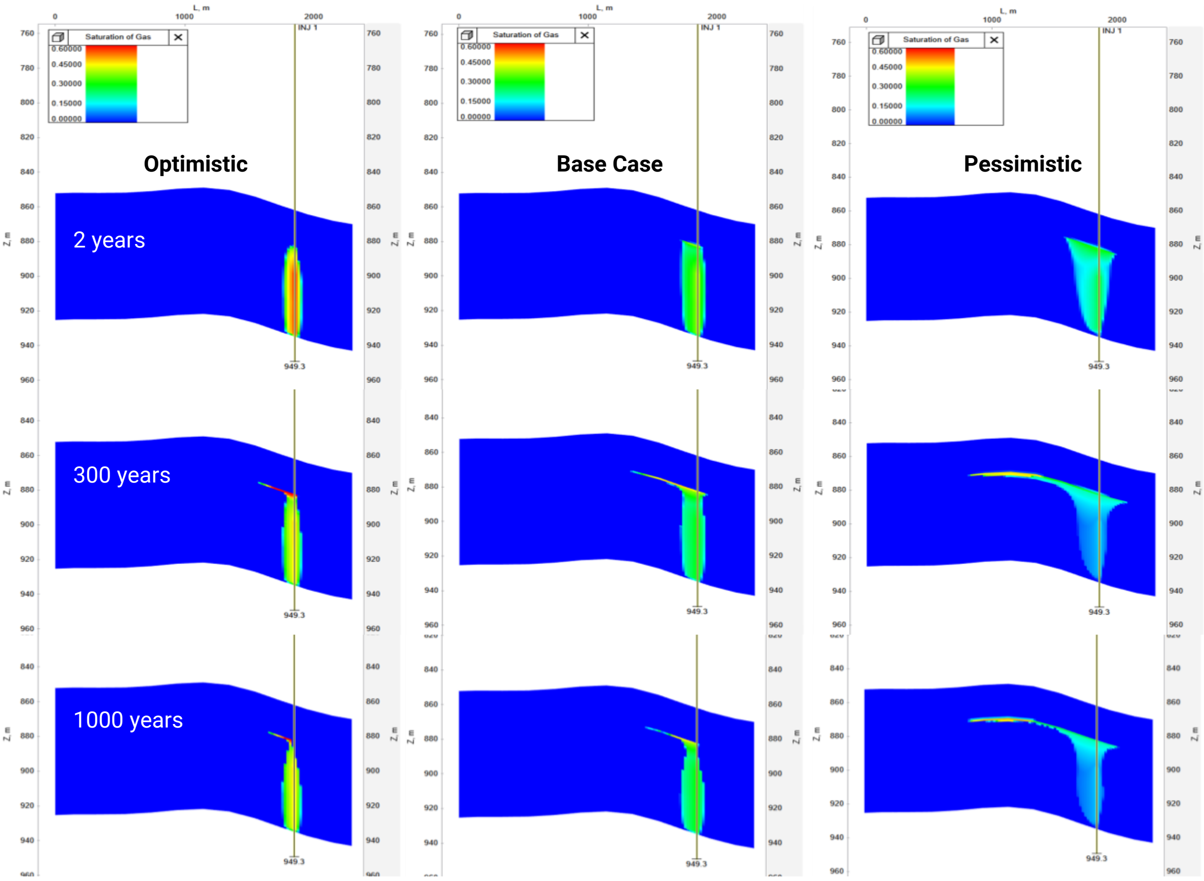

Figure 3 *Simulated free-phase CO_2 saturation distribution for optimistic, base-case, and pessimistic relative permeability scenarios at the end of 2 years of injection and after 300 and 1,000 years of post-injection migration.*

The trapping partitioning results clearly demonstrate that relative permeability uncertainty strongly controls the CO_2 trapping evolution and long-term balance between residual, dissolved, and mobile CO_2 phases.

Immediately after injection, all scenarios exhibit a rapid decline in mobile (free) CO_2 due to buoyancy redistribution and the onset of capillary trapping. However, the magnitude and persistence of mobile CO_2 differ significantly between cases. The pessimistic scenario retains the largest fraction of free CO_2 throughout the simulation period, indicating weaker capillary immobilization and sustained plume mobility. In contrast, the optimistic case shows the most rapid reduction in mobile CO_2, reflecting stronger residual trapping and earlier loss of gas-phase connectivity.

Residual trapping exhibits the clearest separation among scenarios. The optimistic case consistently maintains the highest quantity of CO_2 trapped in the gas phase (residual trapping), demonstrating the impact of higher residual gas saturation (S_{gr}) and stronger hysteresis during imbibition. The base case follows an intermediate trend, while the pessimistic scenario shows the lowest residual trapping efficiency, leaving a greater proportion of CO_2 potentially mobile over long timescales.

Solubility trapping also varies systematically. Dissolved CO_2 increases progressively in all cases, but the pessimistic scenario shows the highest dissolved fraction at late time due to its larger plume footprint and greater brine contact volume. Nevertheless, this increased dissolution does not compensate for the reduced residual trapping, as the mobile CO_2 fraction remains comparatively elevated.

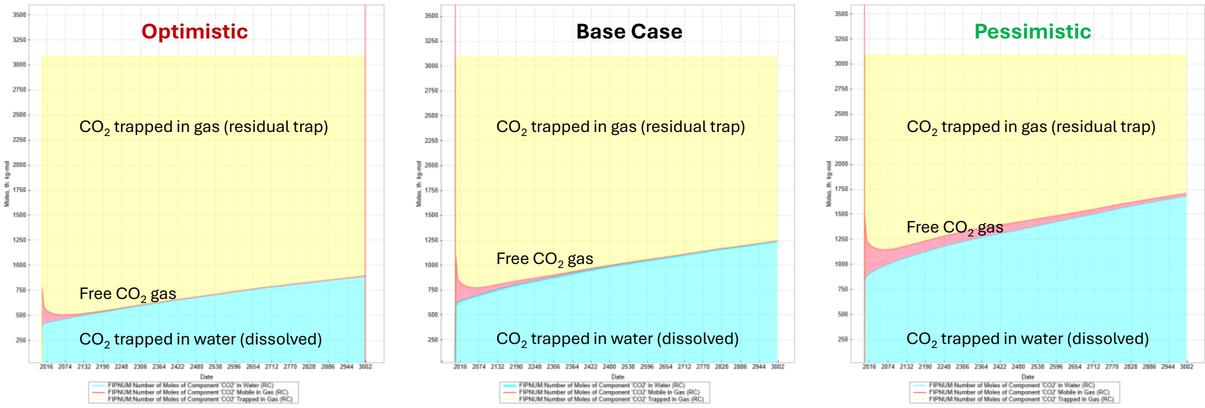

Figure 4 *Effect of relative permeability uncertainty on CO_2 trapping mechanisms over 1,000 years.*

After 1,000 years, the optimistic case is dominated by residual trapping with minimal mobile CO_2, representing the most secure long-term storage configuration. The pessimistic case, although exhibiting substantial dissolution, retains the highest mobile CO_2 fraction, implying lower containment security. These results confirm that relative permeability parameters—particularly S_{gr} and CO_2 endpoint mobility—govern the partitioning between structural, residual, and solubility trapping over millennial timescales.

Conclusions

This study demonstrates that uncertainty in CO_2–brine relative permeability has a decisive influence on plume migration, trapping mechanisms, and long-term storage security. Simulations using optimistic, base, and pessimistic relative permeability scenarios reveal that even small variations in endpoint permeability, irreducible water saturation, and residual gas saturation lead to markedly different plume geometries and trapping efficiency. The pessimistic case results in faster plume migration, greater lateral spread, and a persistently higher mobile CO_2 fraction, indicating lower containment security. In contrast, the optimistic scenario yields compact plumes, stronger residual trapping, and enhanced dissolution, supporting more stable long-term storage. These findings underscore the need for robust, relative permeability uncertainty model when evaluating and designing geological CO_2 storage projects.

Acknowledgements

The authors gratefully acknowledge Rock Flow Dynamics for providing access to the tNavigator software used in this study and for granting permission to publish the results.

References

Akbar, M.N.A., Jenei, B., Lakos, M., Steffens, B., Kulaksiz, S. and Ganzer, L. [2026]. *Assessing the impact of relative permeability uncertainty on geological CO_2 storage using SCAL modeling and numerical simulation.* Proceedings of the SPE Europe Subsurface Conference 2026, SPE-231936-MS.

Jenei, B., Lakos, M., Kulasksiz, S., Steffens, B. and Ganzer, L. [2025]. *Numerical investigation of geological CO_2 storage – sensitivity study on saturation functions.* Proceedings of the SPE Europe Energy Conference and Exhibition, 10–12 June 2025, SPE-225574-MS.